taxonomy

MDPI

Article

Genomic and Phylogenetic Characterization of *Prototheca wickerhamii* UTEX 1533 and Related Strains

Alexander L. Kilbo [1], Leon Parker [1], James Price [1], Charles Francis Delwiche [2], Manuel Oliveira [1], Frédéric Destaillats [1,*] and James Casey Lippmeier [1,*]

[1] Checkerspot, Inc., Alameda, CA 94501, USA
[2] Department of Cell Biology and Molecular Genetics, University of Maryland, College Park, MD 20742, USA
* Correspondence: fdestaillats@checkerspot.com (F.D.); clippmeier@checkerspot.com (J.C.L.)

Abstract

Some edible oils are produced by heterotrophic fermentation of *Prototheca*, a genus of non-photosynthetic green algae. Two accessions from the University of Texas Culture Collection of Algae (UTEX) have been used for oil production: UTEX 1435 historically and UTEX 1533 more recently. Because *Prototheca* classification methods have been revised and collection labels may now be unreliable, linking UTEX 1533 to the production and regulatory history of UTEX 1435 requires establishing whether they are the same species. We compared UTEX 1533 with archival UTEX 1435 sequences, related deposits, and six disease-associated ("clinical") isolates using organellar markers, nuclear phylogeny, whole-genome identity, and mitochondrial intron structure. UTEX 1533 matched historical UTEX 1435 at plastid 16S and 23S rRNA, the only available archival loci. UTEX 1533, ATCC 16525 (linked to historical UTEX 1435), and the *P. wickerhamii*-type strain ATCC 16529 shared identical plastid 16S and 23S and mitochondrial *cytb* sequences. These accessions formed a fully supported nuclear group, with 95.82–98.04% whole-genome identity, versus 88.72–89.83% to the clinical isolates. Two mitochondrial introns shared by this group were absent from all six clinical isolates. Cultures supplied as UTEX 1435 in 2017 and 2026 instead matched *P. xanthoriae*. These findings identify UTEX 1533 as *P. wickerhamii*, conspecific with historical UTEX 1435, and suggest a change in material currently distributed under the UTEX 1435 designation.

Keywords: *Prototheca wickerhamii*; *Prototheca moriformis*; UTEX 1533; UTEX 1435; culture provenance; phylogenomics; average nucleotide identity

Check for updates

Academic Editor: Liwei Zhou

Received: 16 October 2026
Revised: 11 November 2026
Accepted: 12 November 2026
Published: 15 November 2026

Copyright: © 2026 by the authors. Licensee MDPI, Basel, Switzerland. This article is an open access article distributed under the terms and conditions of the Creative Commons Attribution (CC BY) license.

1. Introduction

The genus *Prototheca* W.Krüger was established by Krüger in 1894 for two organisms isolated from tree slime flux, with the genus name proposed by Zopf [1]. The original descriptions distinguished *P. zopfii* W.Krüger and *P. moriformis* W.Krüger, organisms that lacked chlorophyll but reproduced in a *Chlorella*-like manner [1,2]. Initially considered fungi, *Prototheca* were subsequently recognized as non-photosynthetic green algae belonging to the Trebouxiophyceae that retain a reduced plastid [3,4]. In 1959, Tubaki and Soneda described *P. wickerhamii* K. Tubaki & M. Soneda from L. J. Wickerham's isolate YB-4330, collected from a lavatory drain in Peoria, Illinois. The authors designated the isolate as the type and noted oil droplets within the cells [5].

For much of this history, species assignments within the genus relied on cell morphology and carbon-source utilization, although these characters did not consistently distinguish

evolutionary lineages [2,4]. Ewing and coworkers [4] provided a molecular reference in 2014 by comparing plastid 16S and 23S ribosomal RNA (rRNA) gene sequences from 23 *Prototheca* strains. Their clade C included UTEX 1435 (hereafter "historical UTEX 1435"; plastid records KM396170 and KM396205), then labeled *P. moriformis*, and ATCC 16529, the type strain of *P. wickerhamii*, along with other strains showing minor differences in their plastid ribosomal sequences. By contrast, SAG 263-11, also labeled *P. wickerhamii*, occupied a separate clade. Subsequent mitochondrial cytochrome b (*cytb*) analysis and type-based taxonomic revision improved species discrimination and recognized SAG 263-11 as *P. xanthoriae* Jagielski, Karnkowska & Dyląg [3,6]. The same revision lectotypified and epitypified *P. moriformis* and placed it in a cluster separate from *P. wickerhamii* [3]. Older sequence records and species names therefore now require interpretation against authenticated reference cultures [7].

During the same period, oleaginous *Prototheca* strains were developed for edible-oil production by heterotrophic fermentation. The earliest industrial lineage originated from historical UTEX 1435 material, which was clonally purified as S376, the same material represented by the archival plastid records of Ewing and coworkers [4]. Generally recognized as safe (GRAS) notices submitted by Solazyme and TerraVia describe genetically engineered derivatives of this lineage producing high-oleic algal oil, S2532 in GRN 000527 and S6697 in GRN 000754, and a stearic- and oleic acid-rich structuring fat, S7737 in GRN 000673 [8–10]. The notices used the historical species designation *P. moriformis* and identified ATCC 16525 as another deposit associated with historical UTEX 1435 [8–10]. The U.S. Food and Drug Administration (FDA) ultimately responded to each notice that it had no questions [11–13].

Whereas historical UTEX 1435 and ATCC 16525 are recorded as deposits of an original isolate designated PR-9 with W. B. Cooke as depositor on 10 April 1966 (Table S2), a second accession, UTEX 1533, underlies the more recent oil-production studies. Both UTEX 1533 and the *P. wickerhamii*-type strain ATCC 16529 are deposits of the isolate YB-4330, which collection records distinguish from PR-9. Parker and coworkers [14] used classical strain improvement of UTEX 1533 to produce oil containing > 86% oleic acid. Zhou and coworkers [15] combined strain improvement of UTEX 1533 with expression of a lysophosphatidic acid acyltransferase to produce a human milk fat analog enriched in *sn*-2 palmitate. More recently, Zhou and coworkers [16] developed a palmitoleic acid-rich oil through the genetic engineering of the same wild-type accession. All three studies referred to UTEX 1533 as *P. moriformis*. That label was adopted because the plastid sequences of UTEX 1533 placed it in clade C of Ewing and coworkers [4], where four of the six strains, including UTEX 1435, were labeled *P. moriformis*. UTEX 1533, however, traces to YB-4330, the type isolate of *P. wickerhamii* [5,17], a species that a *cytb*-based revision has since separated from *P. moriformis* [3].

These parallel uses make it necessary to establish how UTEX 1533 relates to historical UTEX 1435, a relationship that cannot be inferred from accession labels alone. Ewing and coworkers [4] supplied the early molecular basis for that comparison, but their panel included ATCC 16529 rather than UTEX 1533 itself and examined only two loci in the plastid genome. It did not directly establish genome-wide relatedness between the two UTEX accessions. Comparisons must also distinguish the material represented by archival UTEX 1435 sequences from cultures subsequently supplied under the same catalog designation.

Long-read sequencing and improved genome assembly, together with available nuclear and organellar reference genomes, now permit relationships to be examined beyond individual marker genes [17–19]. Here, we extend the framework of Ewing and coworkers [4] by integrating culture provenance, markers from the plastid, nucleus and mitochondrion, single-copy nuclear-gene phylogeny, whole-genome nucleotide identity and mitochondrial

gene and intron structure. We compare UTEX 1533 with archival UTEX 1435 sequences and the reference deposits ATCC 16525 and ATCC 16529. *Prototheca* is widespread in the environment [20], with *P. wickerhamii* the species most often isolated in an aquatic survey [21]. *P. wickerhamii* is also among the species reported to cause protothecosis, a rare opportunistic human infection [20], so we included six clinical isolates in the analysis.

The present study asks whether UTEX 1533 and historical UTEX 1435 are the same species and, if so, where both fall within the genomic diversity of *P. wickerhamii*, using six clinical isolates for comparison.

2. Materials and Methods

2.1. Cultures, Provenance and Reference Sequences

UTEX 1533 was obtained from the Culture Collection of Algae at the University of Texas at Austin (UTEX) in 2017, confirmed to be axenic and clonally isolated. The retained wild-type isolate, designated UTEX 1533 (2017), was sequenced in 2025. A second UTEX 1533 culture was obtained independently from UTEX in 2026 and designated UTEX 1533 (2026) to confirm the identity of UTEX 1533 (2017). ATCC 16529, the *P. wickerhamii*-type strain, was represented by its published genome (JADZLO01) [17]. ATCC 16525 was obtained and sequenced in 2026.

Historical UTEX 1435 sequences are the archival plastid records KM396170 (16S) and KM396205 (23S) of Ewing and coworkers [4]. These archival records were distinguished from the UTEX 1435 (2017 culture) and UTEX 1435 (2026 culture), the cultures received from the collection under that accession in 2017 and 2026. They were evaluated separately (Section 3.1) and were not used as genomic proxies for historical UTEX 1435. No historical UTEX 1435 nuclear genome, *cytb* sequence, or 18S sequence was publicly available. ATCC 16525 therefore served as the provenance-linked comparator for those analyses.

To show how UTEX 1533 and the reference deposits ATCC 16525 and ATCC 16529 relate to the genomes of *P. wickerhamii* associated with human infections, we used a panel of six clinical isolates: ATCC 30395, HMC1, UVCC 0001, InPu-22_FZ, PW26 and PWS1. These isolates had accessible genome data and a clinical source documented in a publication or repository record. The panel was assembled from genomes identified at the time of analysis. Other public genomes of clinical isolates exist and were not evaluated, so the panel is not exhaustive. Published genomes were used where available [19,22]. ATCC 30395 was assembled from public reads SRR32946134. Clinical provenance was taken from the associated publications and repository records [23]. The comparison therefore comprised ten genomes: four from the production-lineage reference group, comprising UTEX 1533 (2017), UTEX 1533 (2026), ATCC 16525 and ATCC 16529, and six clinical isolates. This group designation refers to the wild-type and reference cultures, not to engineered production strains. Assembly statistics and provenance are provided in Tables S1 and S2.

2.2. Genome Assembly and Phylogenetic Analysis

Genomic DNA from UTEX 1533 (2017), UTEX 1533 (2026), ATCC 16525 and UTEX 1435 (2026 culture) was isolated from cells grown on a defined minimal medium plate using the Quick-DNA Fungal/Bacterial Miniprep Kit (Zymo Research, Irvine, CA, USA) according to the manufacturer's instructions. Purified DNA was sequenced with Oxford Nanopore technology using the company's proprietary sequencing methods (Angstrom Innovation, Berkeley, CA, USA), and the resulting sequences were assembled with Flye [24] and polished with Medaka [25]. Duplicate contigs were removed with purge_dups [26] from both UTEX 1533 assemblies and UTEX 1435 (2026 culture). The UTEX 1533 (2026) and UTEX 1435 (2026 culture) assemblies were scaffolded with RagTag [27]. The UTEX 1435 (2017 culture) genome was assembled from PacBio and Illumina reads using FAL-

CON, PBJelly, and Illumina-based correction [28,29] (Supplementary Method S1). ATCC 30395 reads were trimmed with fastp [30], assembled *de novo* with SPAdes [31], and processed with purge_dups. Completeness was assessed in genome mode with Benchmarking Universal Single-Copy Orthologs (BUSCOs) v6.1.0 and chlorophyta_odb12, containing 1523 reference genes [32].

Plastid 16S and 23S rRNA, mitochondrial *cytb*, and nuclear 18S rRNA sequences were recovered by BLASTN or from annotated GenBank records [33]. Alignments were generated with MAFFT and trimmed with trimAl [34,35]. Maximum-likelihood trees were inferred with IQ-TREE 3 and ModelFinder-selected models [36,37], with 1000 Shimodaira-Hasegawa-like approximate likelihood ratio tests (SH-aLRT) and 1000 ultrafast bootstrap replicates [38,39]. The plastid 23S tree used a fixed GTR + G4 model because ModelFinder and the other fixed models tested gave no support within the cluster of near-identical sequences. The 30-sequence 18S alignment was trimmed to 1711 positions, mainly by removing introns. Identities excluded columns containing a gap in either sequence. ATCC 16529 was represented by the cloned 18S record MF163504 [3]. UTEX 1533 (2026) was represented in the tree by the class A sequence from the UTEX 1533 (2017) assembly (Supplementary Methods S2). Identities of the UTEX 1435 cultures to *P. xanthoriae* reference records were calculated from pairwise BLASTN alignments, also excluding gap columns (Table S3).

Nuclear supermatrices retained complete single-copy BUSCOs present in every genome and were analyzed with one partition per gene: 115 genes and 136,406 positions across 17 taxa, and 253 genes and 302,454 positions across 14 taxa after omitting HMC1, ATCC 30395, and UVCC 0001, the three clinical assemblies with the lowest BUSCO completeness (66.7%, 68.9% and 74.7%; Table S1). *P. bovis* Jagielski, Karnkowska & Dyląg and *P. ciferrii* Negroni & Blaisten were represented by PacBio assemblies of the non-type isolates SH08 and SH13 [40], which are less fragmented than the type-strain assemblies [41]. The gene set was divided once at random into two halves, each analyzed separately, and relationships not consistently recovered across the halves are shown with dashed branches.

2.3. Genome Identity and Mitochondrial Structure

Whole-genome average nucleotide identity was calculated with OrthoANI, implemented in pyorthoani, using corresponding 1020 bp fragments of the nuclear assemblies [42]. All pairwise values were summarized within and between the two groups. Comparisons excluding the fragmented HMC1 and ATCC 30395 assemblies were examined separately. Mitochondrial gene content and order were compared after annotation transfer from the ATCC 16529 mitochondrial genome [7]. Type-strain mitochondrial genomes of other species were taken from Wibberg and coworkers [18]. The presence or absence of two introns in the mitochondrial large subunit rRNA gene (*rnl*) was checked against mitochondrial and complete assemblies and against unassembled ATCC 30395 reads (Supplementary Methods S3). Additional procedures are given in the Supplementary Methods. Software versions and parameters are listed in Table S4.

3. Results

3.1. Historical UTEX 1435 and Marker-Sequence Identity

UTEX 1533 (2017) matched the historical UTEX 1435 plastid 16S and 23S rRNA gene records over their complete available lengths, 1388 and 531 bp, respectively, without substitutions, insertions, or deletions. ATCC 16525 had the same plastid 16S and 23S sequences. UTEX 1533 (2017), ATCC 16525, and the *P. wickerhamii*-type strain ATCC 16529 were also identical at mitochondrial *cytb*. Nuclear 18S rRNA genes occur in multiple, non-identical copies, so 18S identities reflect copy sampling as well as strain diver-

gence and are treated here as corroborative (Supplementary Methods S2). At nuclear 18S, UTEX 1533 (2017) matched ATCC 16525 but differed from the cloned ATCC 16529 record MF163504 at 22 of 1708 compared positions (98.71%; Table 1). Both plastid trees placed the archival record, both UTEX 1533 cultures and the ATCC comparators, together, apart from SAG 263-11 (Figure 1; Figure S1).

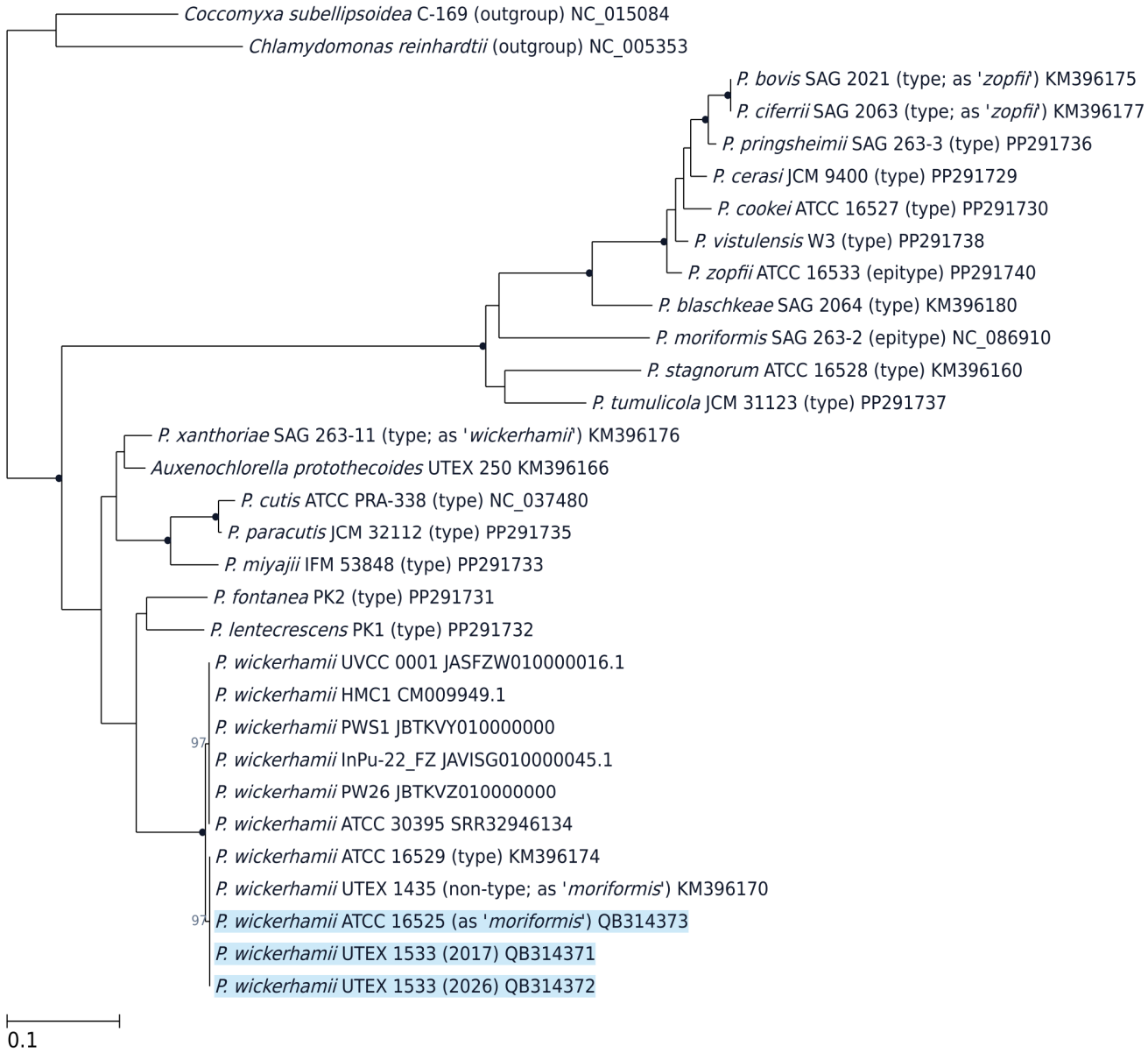


Figure 1. Plastid 16S rRNA phylogeny. Maximum-likelihood tree including all six clinical isolates. Historical UTEX 1435 is represented by KM396170. The UTEX 1435 (2017 culture) and UTEX 1435 (2026 culture) are not included in the tree (Table S3). Both UTEX 1533 cultures, ATCC 16525, ATCC 16529, and the archival record form a terminal cluster. Where a tree tip reads ” as ‘...’ ”, the strain is placed under a species classification supported by this study, and the name in quotes (e.g., as ‘moriformis’) is the catalog or deposited name. Outgroups are *Coccomyxa subellipsoidea* C-169 and *Chlamydomonas reinhardtii*. Numbers show ultrafast bootstrap support of at least 95%, and filled circles denote 100%. The scale denotes substitutions per site.

Table 1. Marker-sequence identities to UTEX 1533 (2017).

Comparator	Plastid 16S (%)	Plastid 23S (%)	Mitochondrial *cytb* (%)	Nuclear 18S (%)
Historical UTEX 1435	100	100	ND	ND
ATCC 16525	100	100	100	100
ATCC 16529 (type; 18S clone)	100	100	100	98.71
UTEX 1533 (2026), assembled sequence	100	100	100	97.37
UTEX 1533 (2026), 18S read class A (vs. 2017 class A)	–	–	–	100 *
Clinical isolates	99.35	98.87	99.74	96.26–96.90

Historical UTEX 1435 is represented by KM396170 (plastid 16S, 1388 bp) and KM396205 (plastid 23S, 531 bp). ATCC 16529 is represented by KM396174 (16S), KM396182 (23S), and the cloned nuclear 18S sequence MF163504. Organellar identities were calculated over the available sequence lengths. Nuclear 18S identities used a trimmed alignment of 1711 positions across 30 sequences. All identities exclude alignment columns containing gaps in either sequence. Nuclear 18S rRNA genes occur in multiple, non-identical copies. Genome assemblies report a consensus sequence, whereas a cloned PCR product represents a single copy, so 18S identity may reflect copy sampling as well as divergence between strains. Raw reads from both UTEX 1533 cultures contain the same two 18S sequence classes (Supplementary Methods S2). The UTEX 1533 (2017) assembly retained class A, whereas the UTEX 1533 (2026) assembly retained class B and one chimeric copy, accounting for its 97.37% identity. The ATCC 16529 clone differed at 22 of 1708 compared positions, and the UTEX 1533 (2026) assembly at 45 of 1710 positions. * identity was calculated from majority-base calls, excluding four positions in class A where neither nucleotide was clearly predominant. ND, no historical sequence available; –, not applicable. The UTEX 1435 (2017 culture) and UTEX 1435 (2026 culture) are not the historical comparator (Section 3.1).

The UTEX 1435 (2026 culture) was identical to the *P. xanthoriae*-type strain SAG 263-11 at plastid 16S and 23S and *cytb*, and 100.00% identical across the plastid and mitochondrial genomes (Table S3). Its nuclear 18S, ITS, and partial LSU sequences were 99.58–99.94% identical to *P. xanthoriae* records. The UTEX 1435 (2017 culture) assembly recovered only 16% of the plastid and 13% of the mitochondrial genome, and these fragments were 99.80% and 99.74% identical to SAG 263-11. The UTEX 1435 (2026 culture) shared 73.5% OrthoANI with UTEX 1533 (2017), far below identity within the production-lineage reference group and below the 79.2% shared by *P. bovis* SH08 and *P. ciferrii* SH13 [40]. Neither culture was therefore used as a genomic proxy for historical UTEX 1435. The historical comparison remained direct at the two archival plastid loci and provenance-linked through ATCC 16525 at the other loci and whole-genome level.

The clinical isolates also shared high marker identities with UTEX 1533 (2017): 99.35% for 16S, 98.87% for 23S, 99.74% for *cytb*, and 96.26–96.90% for nuclear 18S on the trimmed alignment (Table 1). The *cytb* tree provided little resolution among the ten genomes (Figure S2).

3.2. Multicopy 18S Variation in the Two UTEX 1533 Cultures

The two UTEX 1533 acquisitions, obtained nine years apart, were identical at 16S, 23S, and *cytb*. Their assembled 18S sequences differed at 45 of 1710 compared positions on the trimmed alignment (97.37% identity). Raw reads nevertheless contained the same two 18S sequence classes, A and B, in about a 54:46 ratio (Supplementary Methods S2). The UTEX 1533 (2017) assembly retained class A, whereas the UTEX 1533 (2026) assembly retained class B and one chimeric copy. The apparent difference between cultures therefore likely reflects which 18S copies each assembly retained.

Using class A for UTEX 1533 (2026), the 18S tree recovered the four production-lineage sequences together at 99.4% SH-aLRT and 99% ultrafast bootstrap support (Figure S3). The 30-sequence, 1711-position trimmed alignment contained 508 parsimony-informative positions. The 22-position difference from the cloned ATCC 16529 sequence was smaller than the 45-position difference between assemblies of the two UTEX 1533 cultures.

3.3. Assembly Characteristics of the Comparison Panel

The four production-lineage assemblies ranged from 16.51 to 20.18 Mb, with 17–187 contigs, contig N50 values of 169 kb to 1.58 Mb and BUSCO completeness of 71.1–79.9% (Table S1). PW26 and PWS1 had 17 and 14 contigs, respectively, and N50 values of 1.64 Mb, with 80.2% and 79.2% BUSCO completeness. Completeness near 80% therefore does not by itself indicate an incomplete assembly. HMC1 and ATCC 30395 contained 3774 and 3398 contigs, with N50 values of 31 and 11 kb and completeness of 68.9% and 66.7%. HMC1 had a 27.7 Mb assembly with 22.8% duplicated BUSCO genes. These two assemblies were evaluated separately in OrthoANI sensitivity analyses. The reduced nuclear analysis also omitted UVCC 0001 (74.7% complete). UTEX 1533 (2017) was 16.68 Mb in 35 contigs, versus 20.18 Mb in 187 contigs for UTEX 1533 (2026), and ATCC 16525 was 16.51 Mb in 17 contigs. The non-type *P. bovis* SH08 and *P. ciferrii* SH13 nuclear assemblies contained 53 and 96 contigs, respectively. The UTEX 1435 (2017 culture) and UTEX 1435 (2026 culture) assemblies contained 21,972 and 148 contigs, respectively, with 57.5% and 77.5% complete BUSCO genes. Their exclusion as historical comparators was based on marker identity, not assembly quality.

3.4. Nuclear Phylogeny and Whole-Genome Identity

All six pairwise comparisons among the four production-lineage genomes fell between 95.82% and 98.04% OrthoANI, with a mean of 96.66%. All 15 clinical-isolate comparisons fell between 96.99% and 98.43%, with a mean of 97.57%. In contrast, the 24 between-group comparisons ranged from 88.72% to 89.83%, with a mean of 89.50% (Table 2; Figures 2 and S4). No value occurred between 89.83% and 95.82%, leaving a 5.99-percentage-point interval separating the within-group and between-group ranges.

Table 2. Whole-genome identity within and between the two groups.

Comparison	Genome Pairs (n)	OrthoANI Range (%)	Mean (%)
Among four production-lineage genomes	6	95.82–98.04	96.66
Among six clinical isolates	15	96.99–98.43	97.57
Among clinical isolates, excluding HMC1	10	96.99–97.46	97.25
Between the two groups	24	88.72–89.83	89.50

The production-lineage genomes are UTEX 1533 (2017), UTEX 1533 (2026), ATCC 16525 and ATCC 16529. The six clinical isolates are ATCC 30395, HMC1, UVCC 0001, InPu-22_FZ, PW26 and PWS1. Pair counts are the numbers of unique comparisons implied by the specified group sizes, and the HMC1-excluded row is a sensitivity subset, not an additional primary group. Ranges and means are those reported for the all-by-all OrthoANI matrix. No comparison fell between 89.83% and 95.82%.

HMC1 accounts for all the highest within-clinical values (98.01–98.43%). Because this short-read assembly is fragmented and contains 22.8% duplicated BUSCO genes (Section 3.3), its effect was examined separately. Without HMC1, the clinical isolates shared 96.99–97.46% (mean 97.25%). The between-group range of 88.72–89.83% was unchanged, whether HMC1 was excluded alone or together with ATCC 30395. ATCC 16529 gave the lowest within-group values (95.82–96.32%), although it derives from the same recorded isolate as UTEX 1533 (Section 4.3).

The 115-gene nuclear supermatrix, comprising 136,406 positions across 17 taxa, recovered the four production-lineage genomes and the six clinical isolates as separate clades, each with 100% SH-aLRT and ultrafast bootstrap support (Figure 3a). Omitting HMC1, ATCC 30395, and UVCC 0001 increased the retained dataset to 253 genes and 302,454 positions across 14 taxa. The four production-lineage genomes and the three remaining clinical iso-

lates, InPu-22_FZ, PWS1 and PW26, again formed separate clades at 100% by both measures (Figure 3b). The two UTEX 1533 cultures paired at 100% in both analyses. Increasing the shared gene set therefore did not change the separation of the two groups. Branching orders not consistently recovered across the two random gene halves are shown as dashed branches and do not affect these supported groupings.

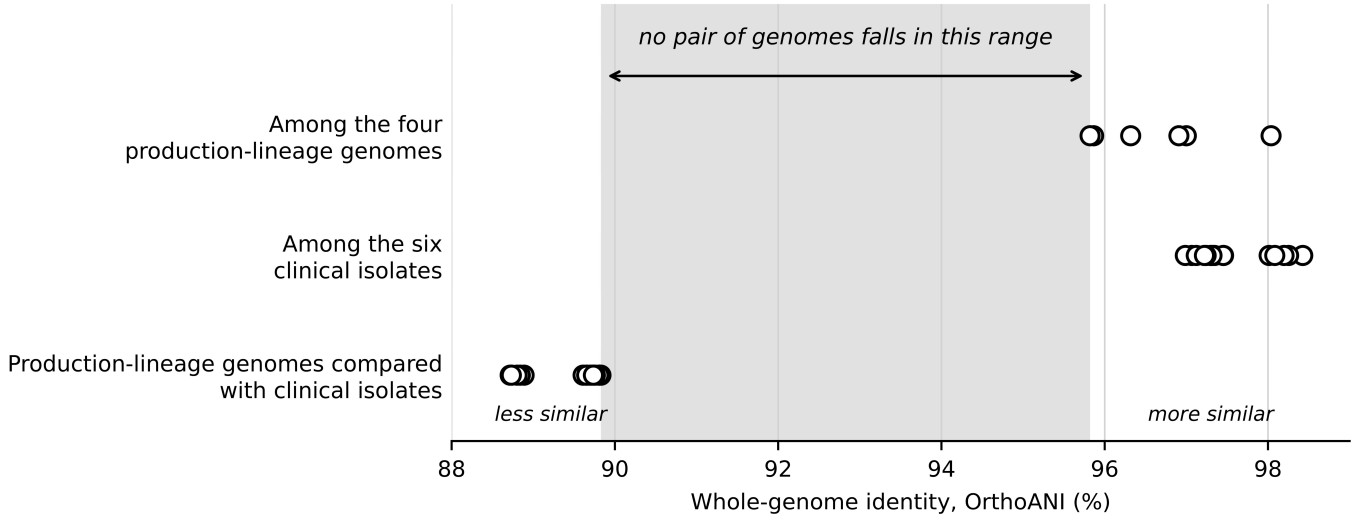


Figure 2. Separation of within-group and between-group whole-genome identities. Each circle represents one of the 45 unique pairs among the ten genomes. Overlapping values may obscure individual circles. The upper two rows are comparisons within the four production-lineage genomes and within the six clinical isolates. The bottom row contains comparisons between groups. The shaded band marks the interval containing no pairwise value. The corresponding ten-genome matrix is given in Figure S4.

3.5. Mitochondrial Structure and Sequence Validation

Mitochondrial gene order was conserved across the ten genomes. The four production-lineage genomes had three *rnl* introns containing *orf148*, *orf210*, and *orf236*, whereas all six clinical isolates had only the *orf236* intron (Figure 4). The two additional introns measured 1073 and 1021 bp in UTEX 1533 (2017). Both were recovered at full length and 100% identity in all four lineage genomes, but neither returned a full or partial match in any clinical mitochondrial or complete genome assembly.

A 620 bp query sequence joining the *rnl* sequence across both intron-free positions, including the intervening 20 bp coding segment, aligned continuously at 99.8% identity in all six clinical isolates. The matches lay at least 1.7 kb from the ends of single-contig mitochondrial assemblies measuring 52.1–52.4 kb, compared with approximately 53.9 kb in UTEX 1533 (2017).

Unassembled ATCC 30395 reads provided 321 and 385 exact 30-base matches across the two intron-free junctions and 694 matches to an *rnl* control sequence. No read contained the interior of either intron or an intron-exon junction. Raw reads from the other five clinical isolates were not examined.

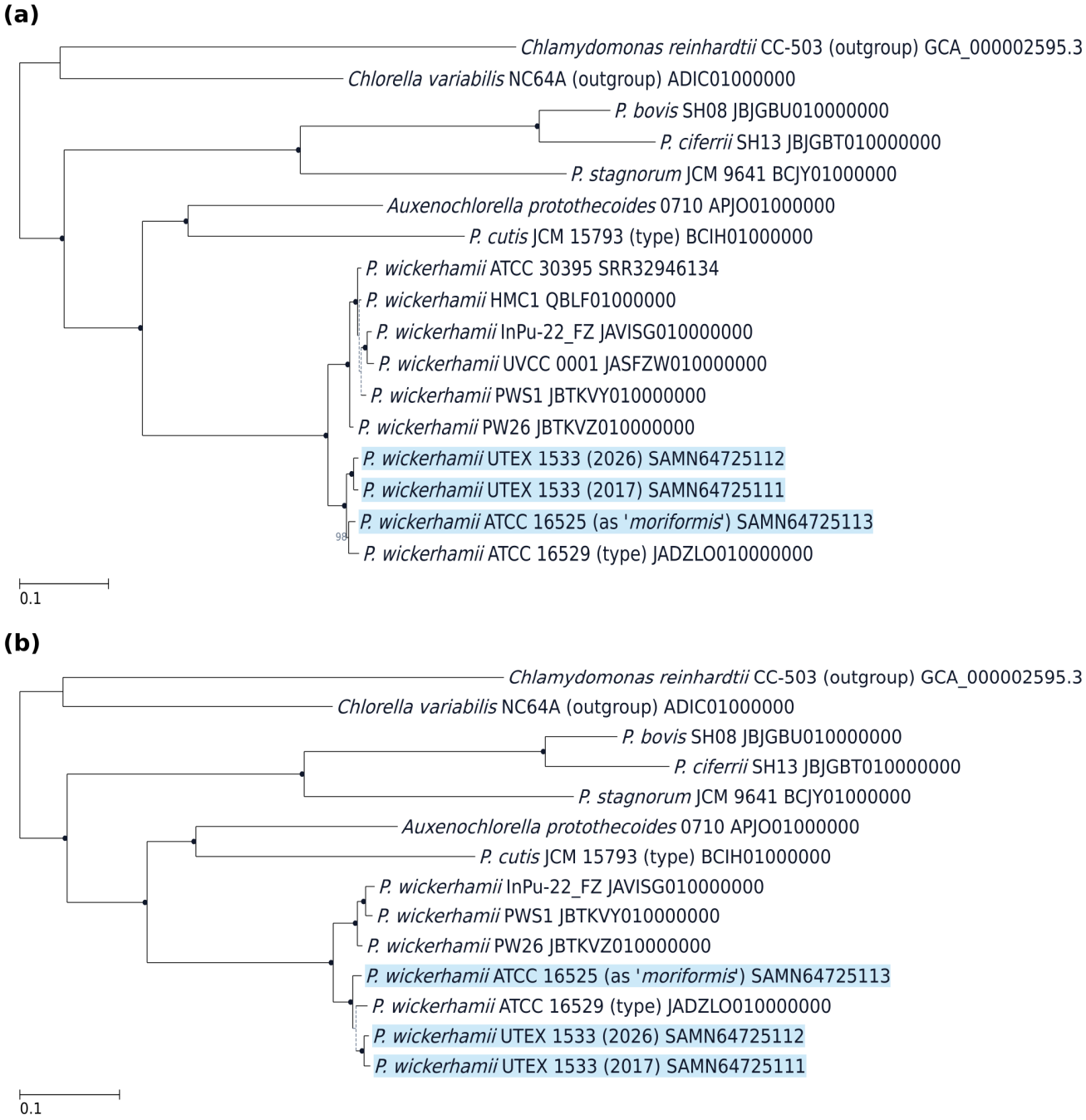


Figure 3. Nuclear phylogeny of the production-lineage reference group and clinical isolates. (**a**) 115 complete single-copy BUSCO genes, 136,406 aligned positions and 17 taxa. (**b**) 253 genes, 302,454 positions and 14 taxa, omitting HMC1, ATCC 30395, and UVCC 0001. The four production-lineage genomes, the clinical isolates retained in each panel, and the UTEX 1533 pair each receive 100% SH-aLRT and ultrafast bootstrap support. Numbers show ultrafast bootstrap support of at least 95%, and filled circles denote 100%. Dashed branches indicate relationships not consistently recovered when the gene set was divided once at random into two halves. Tip labels identify nuclear assemblies or source reads. Genomes sequenced in this study are identified by BioSample (SAMN64725111–SAMN64725113). Tip labels are as in Figure 1. *Chlamydomonas reinhardtii* CC-503 and *Chlorella variabilis* NC64A are outgroups. Scales denote substitutions per site.

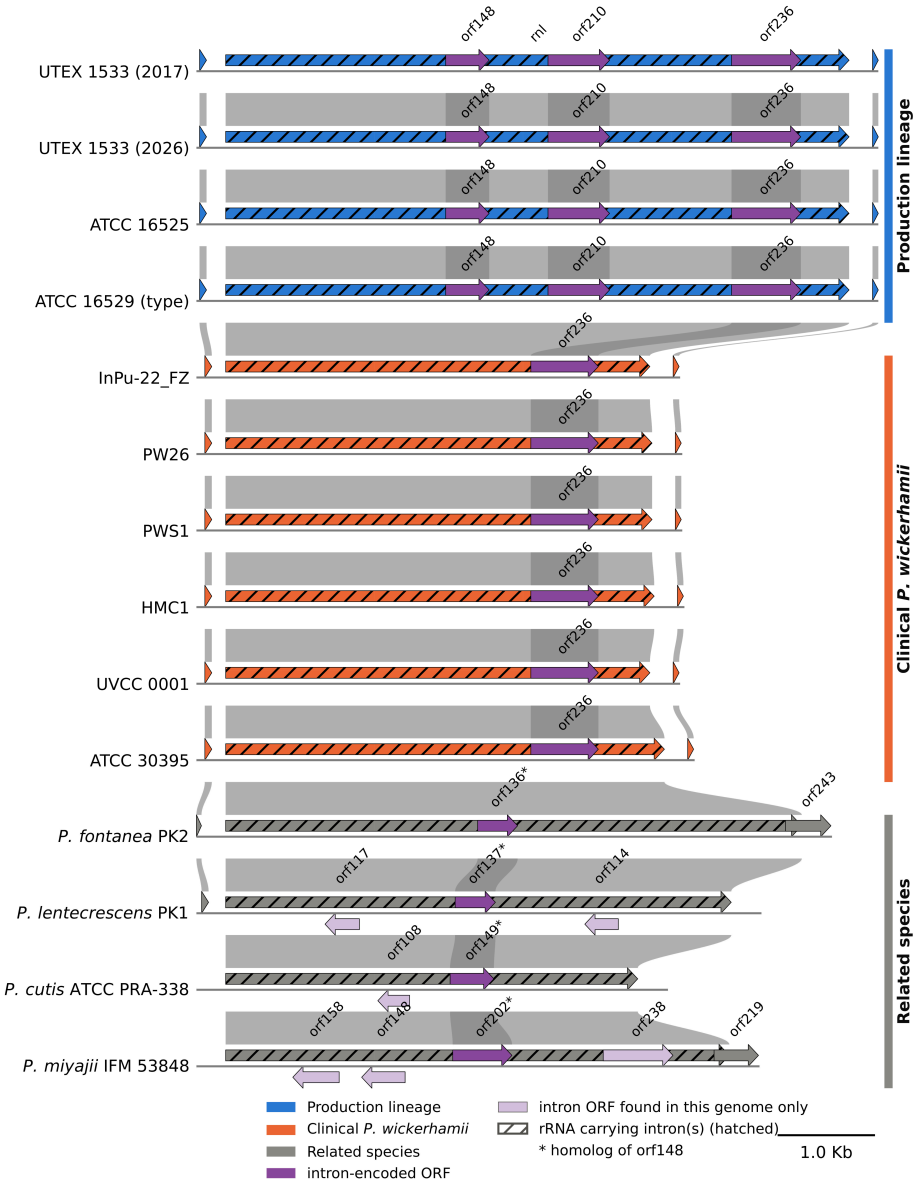


Figure 4. Mitochondrial *rnl* structure. The four production-lineage genomes (top) have introns containing *orf148*, *orf210*, and *orf236*, and the six clinical isolates (middle) retain only the *orf236* intron. Four other *Prototheca* species are shown for comparison. Hatched bars denote *rnl* containing introns, purple arrows intron-associated open reading frames, and gray bands corresponding sequences. An asterisk identifies an open reading frame homologous to *orf148*. Scale bar, 1.0 kb.

4. Discussion

4.1. Taxonomic Relationship and Accession-Associated Material

Linking UTEX 1533 to the production and regulatory history of historical UTEX 1435 required establishing whether the two accessions are the same species. The combined evidence places UTEX 1533 and historical UTEX 1435 in the same species, although they derive from different recorded isolates. Archival plastid sequences provide the direct historical comparison. ATCC 16525 connects those sequences to a separately maintained PR-9 deposit, and the nuclear and mitochondrial data place that comparator with UTEX 1533 and ATCC 16529. The association with the *P. wickerhamii*-type strain supplies the nomenclatural anchor [3,5,17]. UTEX 1533 is therefore conspecific with the UTEX 1435 analyzed by Ewing and coworkers [4].

The UTEX 1435 (2017 culture) and UTEX 1435 (2026 culture) represent a different organism distributed under the same catalog number. Their marker identities to SAG 263-11 are consistent with *P. xanthoriae* as circumscribed by Jagielski and coworkers [3], not with historical UTEX 1435. An apparent change in accession-associated material is the explanation most consistent with the data. Labeling error or cross-contamination could account for it, but the records do not establish the mechanism, timing, or point of occurrence.

4.2. Complementary Resolution of Marker and Genome Analyses

The marker results show both the value and the limits of the early plastid framework. Identity at the historical loci connects the present analysis to Ewing and coworkers [4], but high identities among the clinical and production-lineage genomes show why conserved markers alone provide limited resolution within this panel. Mitochondrial *cytb* is the marker used to delimit *Prototheca* species [3,6]. The 99.74% *cytb* identity between the two groups exceeds the 98.8% minimum that Jagielski and coworkers observed among *P. wickerhamii* strains [3]. Both groups therefore belong to *P. wickerhamii*, and the genomic separation described below lies within the species under the current classification paradigm.

The 18S results show the effect of sampling a multicopy gene. MF163504 represents one cloned ATCC 16529 copy, whereas the UTEX assemblies reduce multiple copies to one sequence. Its 22-position difference from UTEX 1533 (2017) is smaller than the 45-position difference between assemblies of two cultures with the same sequence class. The type-strain difference is therefore compatible with copy sampling and does not indicate a separate lineage. Representing UTEX 1533 (2026) by shared class A recovers the four-culture group at 99% bootstrap support. Jagielski and coworkers likewise found cloned 18S sequences from a single *P. wickerhamii* strain differing at up to 71 positions [6].

4.3. Genomic Separation and Mitochondrial Corroboration

The separation of the two groups is supported by nuclear, whole-genome, and mitochondrial evidence. Removing HMC1 and ATCC 30395 leaves the between-group OrthoANI range unchanged. Separately, removing those assemblies and UVCC 0001 increases the nuclear dataset from 115 to 253 genes while retaining full support for both groups. Assembly fragmentation therefore limits the shared gene set without accounting for the observed separation. ATCC 16529 shares only 95.82% OrthoANI with UTEX 1533 (2017), although both derive from YB-4330, whereas ATCC 16525, recorded as a different isolate, shares 96.91%. This pattern is consistent with an assembly effect. UTEX 1533 (2017) is diploid (Figure S5), as expected from the heterozygosity reported for other *P. wickerhamii* genomes [43] and the vegetative diploidy of the related genus *Auxenochlorella* [44]. Each assembly reduces both haplotypes to one consensus, choosing between them region by region. ATCC 16529 was assembled from PacBio and Illumina reads, and the other three production-lineage genomes from Nanopore reads, so their consensus choices need not agree. ATCC 16529 is also about 1 percentage point lower than the other three against every genome, including the clinical isolates (88.72–88.89% versus 89.61–89.83%; Figure S4), an offset that cannot reflect relatedness to UTEX 1533. Even the two UTEX 1533 assemblies, obtained nine years apart, share only 98.04%. In *Auxenochlorella*, likely sister cultures maintained at UTEX and CCAP also differ by loss of heterozygosity that arose during laboratory culture [44]. Fine-scale OrthoANI differences within either group therefore do not measure divergence between isolates. No whole-genome identity threshold for species has been established in *Prototheca*. For scale, *P. bovis* SH08 and *P. ciferrii* SH13, the most similar pair of named species in this dataset, share 79.2%, well below the 88.72–89.83% between the two *P. wickerhamii* groups.

Differences in cultivation, handling and storage can be assessed indirectly from comparisons among the genomes available. The two UTEX 1533 cultures, acquired nine years apart, were identical at plastid 16S and 23S and mitochondrial *cytb* and share 98.04% OrthoANI. ATCC 16529 and UTEX 1533 derive from the same isolate and were maintained separately by two collections, and they share 95.82–96.32% (Figure S4). These pairs bound the variation expected from differences in handling, storage and time in culture, together with consensus assembly of a diploid genome, sequencing error and read depth. Their shortfall from 100% is 1.96–4.18 points, whereas the 88.72–89.83% between the two groups falls 10.17–11.28 points short. The clinical isolates, which were obtained from human infections, were assembled from different source data and at varying quality (Table S1), yet they share 96.99–98.43% with one another, a range similar to that of the production-lineage genomes. The separation of the groups is therefore more than twice the largest shortfall attributable to assembly, source data, or culture history. Because no OrthoANI threshold has been established for *Prototheca* species, and *cytb* places both groups in *P. wickerhamii*, these data do not settle whether the separation merits taxonomic recognition. Additional isolates and defined criteria would be needed.

The *rnl* intron pattern supplies a structural character independent of marker-sequence identity. Continuous intron-free junctions in all six clinical assemblies and supporting raw reads for ATCC 30395 strengthen the interpretation beyond annotation alone. However, introns with homing-endonuclease open reading frames occur throughout *Prototheca* mitochondria [18], and *orf148* homologs also occur in the other species shown in Figure 4. The pattern is therefore a lineage-associated character in this panel, not evidence that the introns determine pathogenicity.

Jian and coworkers [45] re-sequenced 40 clinical isolates from China together with ATCC 16529. Six clinical isolates, including S1 and S931, grouped with ATCC 16529, apart from the remaining 34. That analysis used short reads mapped to the ATCC 16529 assembly, and the data are not public, so those isolates could not be placed relative to the groups defined here. If they fall within the group containing UTEX 1533, the separation reported here applies to the isolates examined and does not divide *P. wickerhamii* into clinical and non-clinical lineages.

5. Conclusions

UTEX 1533 and historical UTEX 1435 are best interpreted as conspecific members of *P. wickerhamii*, together with ATCC 16529 and ATCC 16525. The UTEX 1435 (2017 culture) and UTEX 1435 (2026 culture) are matches to *P. xanthoriae*. The sequence discrepancy is most consistent with a change in the material distributed by the culture collection under that designation. Both nuclear supermatrices recover the production-lineage reference group with full support and unambiguously separate it from the clinical isolates retained in each analysis. Whole-genome identity and mitochondrial intron structure corroborate this separation within the examined panel.

Supplementary Materials: The following supporting information can be downloaded at https://www.mdpi.com/article/10.3390/taxonomy6040072/s1. Method S1: Assembly assessment and comparisons; Method S2: Marker comparisons and multicopy 18S variation; Method S3: Mitochondrial intron validation; Table S1: Sequencing and assembly statistics for the ten genomes and the UTEX 1435 (2017 culture) and UTEX 1435 (2026 culture); Table S2: Culture provenance and clinical sources of the comparison panel; Table S3: Marker-sequence identities of the UTEX 1435 (2017 culture) and UTEX 1435 (2026 culture) to *Prototheca xanthoriae* reference records.; Table S4: Software versions and parameters; Figure S1: Plastid 23S rRNA phylogeny; Figure S2: Mitochondrial *cytb* phylogeny; Figure S3: Nuclear 18S rRNA phylogeny; Figure S4: All-by-all OrthoANI matrix for the ten genomes, ordered by hierarchical clustering; Figure S5: Read-level evidence of diploidy in UTEX 1533 (2017).

Author Contributions: Conceptualization, L.P., A.L.K., C.F.D. and J.C.L.; methodology, A.L.K. and J.C.L.; investigation, J.P.; formal analysis, A.L.K. and L.P.; resources, J.P.; writing—original draft preparation, F.D.; writing—review and editing, L.P., A.L.K., F.D., M.O., C.F.D. and J.C.L.; supervision, J.C.L. All authors have read and agreed to the published version of the manuscript.

Funding: This research received no external funding.

Data Availability Statement: Sequence data generated in this study have been deposited under NCBI BioProject PRJNA1558063. Accessions for UTEX 1533 (2017), UTEX 1533 (2026), ATCC 16525, and UTEX 1435 (2026 culture), respectively, are: BioSamples SAMN64725111, SAMN64725112, SAMN64725113, and SAMN64992527; Oxford Nanopore reads SRR41599651, SRR41599650, SRR41599649, and SRR41686204; plastid genomes QB314371, QB314372, QB314373, and QB328203; and mitochondrial genomes QB328199, QB328200, QB328201, and QB328202. Nuclear genome assemblies have been submitted to GenBank WGS under the corresponding BioSamples.

Conflicts of Interest: A.L.K., L.P., J.P., F.D. and J.C.L. are employees of Checkerspot, Inc., which develops algal oils and related ingredients derived from *Prototheca wickerhamii* UTEX 1533 for commercial applications. C.F.D. declares no conflicts of interest.

References

1. Krüger, W. Kurze Charakteristik einiger niederer Organismen im Saftflusse der Laubbäume. *Hedwigia* **1894**, *33*, 241–266.
2. Pore, R.S. *Prototheca* taxonomy. *Mycopathologia* **1985**, *90*, 129–139. [CrossRef]
3. Jagielski, T.; Bakuła, Z.; Gawor, J.; Maciszewski, K.; Kusber, W.-H.; Dyląg, M.; Nowakowska, J.; Gromadka, R.; Karnkowska, A. The genus *Prototheca* (Trebouxiophyceae, Chlorophyta) revisited: Implications from molecular taxonomic studies. *Algal Res.* **2019**, *43*, 101639. [CrossRef]
4. Ewing, A.; Brubaker, S.; Somanchi, A.; Yu, E.; Rudenko, G.; Reyes, N.; Espina, K.; Grossman, A.; Franklin, S. 16S and 23S plastid rDNA phylogenies of *Prototheca* species and their auxanographic phenotypes. *J. Phycol.* **2014**, *50*, 765–769. [CrossRef] [PubMed]
5. Tubaki, K.; Soneda, M. Cultural and taxonomical studies on *Prototheca*. *Nagaoa* **1959**, *6*, 25–34.
6. Jagielski, T.; Gawor, J.; Bakuła, Z.; Decewicz, P.; Maciszewski, K.; Karnkowska, A. *cytb* as a new genetic marker for differentiation of *Prototheca* species. *J. Clin. Microbiol.* **2018**, *56*, e00584-18. [CrossRef] [PubMed]
7. Bakuła, Z.; Gromadka, R.; Gawor, J.; Siedlecki, P.; Pomorski, J.J.; Maciszewski, K.; Gromadka, A.; Karnkowska, A.; Jagielski, T. Sequencing and analysis of the complete organellar genomes of *Prototheca wickerhamii*. *Front. Plant Sci.* **2020**, *11*, 1296. [CrossRef] [PubMed]
8. Solazyme, Inc. *Dossier in Support of the Generally Recognized as Safe (GRAS) Status of High-Oleic Algal Oil from a Modified Strain of Prototheca moriformis as a Food Ingredient*; GRAS Notice No. GRN 000527; United States Food and Drug Administration: Silver Spring, MD, USA, 2014.
9. TerraVia Holdings, Inc. *Algal Structuring Fat GRAS Notification*; GRAS Notice No. GRN 000673; United States Food and Drug Administration: Silver Spring, MD, USA, 2016.
10. TerraVia Holdings, Inc. *Notification of GRAS Status of High-Oleic Algal Oil*; GRAS Notice No. GRN 000754; United States Food and Drug Administration: Silver Spring, MD, USA, 2017.
11. United States Food and Drug Administration. *Agency Response Letter, GRAS Notice No. GRN 000527: High-Oleic Algal Oil from Prototheca moriformis Strain S2532*; United States Food and Drug Administration: Silver Spring, MD, USA, 2015.
12. United States Food and Drug Administration. *Agency Response Letter, GRAS Notice No. GRN 000673: Algal Fat Derived from Prototheca moriformis (S7737)*; United States Food and Drug Administration: Silver Spring, MD, USA, 2017.
13. United States Food and Drug Administration. *Agency Response Letter, GRAS Notice No. GRN 000754: High-Oleic Algal Oil from Prototheca moriformis Strain S6697*; United States Food and Drug Administration: Silver Spring, MD, USA, 2018.
14. Parker, L.; Ward, K.; Pilarski, T.; Price, J.; Derkach, P.; Correa, M.; Miller, R.; Benites, V.; Athanasiadis, D.; Doherty, B.; et al. Development and large-scale production of high-oleic acid oil by fermentation of microalgae. *Fermentation* **2024**, *10*, 566. [CrossRef]
15. Zhou, X.; Zhao, X.; Parker, L.; Derkach, P.; Correa, M.; Benites, V.; Miller, R.; Athanasiadis, D.; Doherty, B.; Alnozaili, G.; et al. Development and large-scale production of human milk fat analog by fermentation of microalgae. *Front. Nutr.* **2024**, *11*, 1341527. [CrossRef] [PubMed]
16. Zhou, X.; Correa, M.; Athanasiadis, D.; Benites, V.; Doherty, B.; Edy, L.; Piamonte, C.; Eliares, G.; Cornejo, M.; Gong, T.; et al. Development of high palmitoleic (16:1 n-7) acid oil by fermentation of microalgae. *Fermentation* **2026**, *12*, 160. [CrossRef]
17. Bakuła, Z.; Siedlecki, P.; Gromadka, R.; Gawor, J.; Gromadka, A.; Pomorski, J.J.; Panagiotopoulou, H.; Jagielski, T. A first insight into the genome of *Prototheca wickerhamii*, a major causative agent of human protothecosis. *BMC Genom.* **2021**, *22*, 168. [CrossRef] [PubMed]

18. Wibberg, D.; Bakuła, Z.; García-Cunchillos, I.; Gawor, J.; Gromadka, R.; Karnkowska, A.; Bielecki, J.; Jagielski, T. Complete mitochondrial genomes of the *Prototheca* genus: Comparative genomics and evolutionary insights. *BMC Genom.* **2025**, *26*, 766. [CrossRef] [PubMed]
19. Fang, L.; Guo, J.; Ning, Q.; Luo, Y.; Jian, J.; Ning, J. High-quality genome assemblies of two *Prototheca wickerhamii* strains. *Sci. Data* **2026**, *13*, 633. [CrossRef] [PubMed]
20. Lass-Flörl, C.; Mayr, A. Human protothecosis. *Clin. Microbiol. Rev.* **2007**, *20*, 230–242. [CrossRef] [PubMed]
21. Jagielski, T.; Iskra, M.; Bakuła, Z.; Rudna, J.; Roeske, K.; Nowakowska, J.; Bielecki, J.; Krukowski, H. Occurrence of *Prototheca* microalgae in aquatic ecosystems with a description of three new species, *Prototheca fontanea*, *Prototheca lentecrescens*, and *Prototheca vistulensis*. *Appl. Environ. Microbiol.* **2022**, *88*, e01092-22. [CrossRef] [PubMed]
22. Li, J.; He, X.; Guo, H.; Lin, D.; Wu, X.; Chen, B. Complete genome identified of clinical isolate *Prototheca*. *J. Med. Microbiol.* **2024**, *73*, 001914. [CrossRef] [PubMed]
23. Lee, W.-S.; Lagios, M.D.; Leonards, R. Wound infection by *Prototheca wickerhamii*, a saprophytic alga pathogenic for man. *J. Clin. Microbiol.* **1975**, *2*, 62–66. [CrossRef] [PubMed]
24. Kolmogorov, M.; Yuan, J.; Lin, Y.; Pevzner, P.A. Assembly of long, error-prone reads using repeat graphs. *Nat. Biotechnol.* **2019**, *37*, 540–546. [CrossRef] [PubMed]
25. Oxford Nanopore Technologies. Medaka: Sequence Correction Provided by ONT Research, Version 2.2.1. Available online: https://github.com/nanoporetech/medaka (accessed on 10 June 2026).
26. Guan, D.; McCarthy, S.A.; Wood, J.; Howe, K.; Wang, Y.; Durbin, R. Identifying and removing haplotypic duplication in primary genome assemblies. *Bioinformatics* **2020**, *36*, 2896–2898. [CrossRef] [PubMed]
27. Alonge, M.; Lebeigle, L.; Kirsche, M.; Jenike, K.; Ou, S.; Aganezov, S.; Wang, X.; Lippman, Z.B.; Schatz, M.C.; Soyk, S. Automated assembly scaffolding using RagTag elevates a new tomato system for high-throughput genome editing. *Genome Biol.* **2022**, *23*, 258. [CrossRef] [PubMed]
28. Chin, C.-S.; Peluso, P.; Sedlazeck, F.J.; Nattestad, M.; Concepcion, G.T.; Clum, A.; Dunn, C.; O'Malley, R.; Figueroa-Balderas, R.; Morales-Cruz, A.; et al. Phased diploid genome assembly with single-molecule real-time sequencing. *Nat. Methods* **2016**, *13*, 1050–1054. [CrossRef] [PubMed]
29. English, A.C.; Richards, S.; Han, Y.; Wang, M.; Vee, V.; Qu, J.; Qin, X.; Muzny, D.M.; Reid, J.G.; Worley, K.C.; et al. Mind the gap: Upgrading genomes with Pacific Biosciences RS long-read sequencing technology. *PLoS ONE* **2012**, *7*, e47768. [CrossRef] [PubMed]
30. Chen, S.; Zhou, Y.; Chen, Y.; Gu, J. Fastp: An ultra-fast all-in-one FASTQ preprocessor. *Bioinformatics* **2018**, *34*, i884–i890. [CrossRef] [PubMed]
31. Bankevich, A.; Nurk, S.; Antipov, D.; Gurevich, A.A.; Dvorkin, M.; Kulikov, A.S.; Lesin, V.M.; Nikolenko, S.I.; Pham, S.; Prjibelski, A.D.; et al. SPAdes: A new genome assembly algorithm and its applications to single-cell sequencing. *J. Comput. Biol.* **2012**, *19*, 455–477. [CrossRef] [PubMed]
32. Tegenfeldt, F.; Kuznetsov, D.; Manni, M.; Berkeley, M.; Zdobnov, E.M.; Kriventseva, E.V. OrthoDB and BUSCO update: Annotation of orthologs with wider sampling of genomes. *Nucleic Acids Res.* **2025**, *53*, D516–D522. [CrossRef] [PubMed]
33. Camacho, C.; Coulouris, G.; Avagyan, V.; Ma, N.; Papadopoulos, J.; Bealer, K.; Madden, T.L. BLAST+: Architecture and applications. *BMC Bioinform.* **2009**, *10*, 421. [CrossRef] [PubMed]
34. Katoh, K.; Standley, D.M. MAFFT multiple sequence alignment software version 7: Improvements in performance and usability. *Mol. Biol. Evol.* **2013**, *30*, 772–780. [CrossRef] [PubMed]
35. Capella-Gutiérrez, S.; Silla-Martínez, J.M.; Gabaldón, T. TrimAl: A tool for automated alignment trimming in large-scale phylogenetic analyses. *Bioinformatics* **2009**, *25*, 1972–1973. [CrossRef] [PubMed]
36. Wong, T.K.F.; Ly-Trong, N.; Ren, H.; Demotte, P.; Baños, H.; Roger, A.J.; Susko, E.; Bielow, C.; De Maio, N.; Goldman, N.; et al. IQ-TREE 3: Phylogenomic inference software using complex evolutionary models. *Mol. Biol. Evol.* **2026**, *43*, msag117. [CrossRef] [PubMed]
37. Kalyaanamoorthy, S.; Minh, B.Q.; Wong, T.K.F.; von Haeseler, A.; Jermiin, L.S. ModelFinder: Fast model selection for accurate phylogenetic estimates. *Nat. Methods* **2017**, *14*, 587–589. [CrossRef] [PubMed]
38. Guindon, S.; Dufayard, J.-F.; Lefort, V.; Anisimova, M.; Hordijk, W.; Gascuel, O. New algorithms and methods to estimate maximum-likelihood phylogenies: Assessing the performance of PhyML 3.0. *Syst. Biol.* **2010**, *59*, 307–321. [CrossRef] [PubMed]
39. Hoang, D.T.; Chernomor, O.; von Haeseler, A.; Minh, B.Q.; Vinh, L.S. UFBoot2: Improving the ultrafast bootstrap approximation. *Mol. Biol. Evol.* **2018**, *35*, 518–522. [CrossRef] [PubMed]
40. Guo, J.; Ming, Y.; Chen, J.; Xue, Y.; Peng, Y.; Zhu, H.; Jiang, C.; Wu, W. Two high-quality genomes of *Prototheca bovis* strain SH08 and *Prototheca ciferrii* strain SH13. *Sci. Data* **2026**, *13*, 23. [CrossRef] [PubMed]
41. Severgnini, M.; Lazzari, B.; Capra, E.; Chessa, S.; Luini, M.; Bordoni, R.; Castiglioni, B.; Ricchi, M.; Cremonesi, P. Genome sequencing of *Prototheca zopfii* genotypes 1 and 2 provides evidence of a severe reduction in organellar genomes. *Sci. Rep.* **2018**, *8*, 14637. [CrossRef] [PubMed]

42. Lee, I.; Ouk Kim, Y.; Park, S.-C.; Chun, J. OrthoANI: An improved algorithm and software for calculating average nucleotide identity. *Int. J. Syst. Evol. Microbiol.* **2016**, *66*, 1100–1103. [CrossRef] [PubMed]
43. Guo, J.; Jian, J.; Wang, L.; Xiong, L.; Lin, H.; Zhou, Z.; Sonnenschein, E.C.; Wu, W. Genome sequences of two strains of *Prototheca wickerhamii* provide insight into the protothecosis evolution. *Front. Cell. Infect. Microbiol.* **2022**, *12*, 797017. [CrossRef] [PubMed]
44. Craig, R.J.; Dueñas, M.A.; Camacho, D.J.; Gallaher, S.D.; Avendaño-Monsalve, M.C.; Lin, Y.; Blaby-Haas, C.E.; Moseley, J.L.; Merchant, S.S. Targeted genetic manipulation and yeast-like evolutionary genomics in the green alga *Auxenochlorella*. *Plant Cell* **2025**, *37*, koaf259. [CrossRef] [PubMed]
45. Jian, J.; Luo, Y.; Yang, K.; Wang, S.; Guo, J. Resequencing of 41 strains reveals the diversity and adaptation of *Prototheca wickerhamii*. *Algal Res.* **2026**, *96*, 104709. [CrossRef]

Disclaimer/Publisher's Note: The statements, opinions and data contained in all publications are solely those of the individual author(s) and contributor(s) and not of MDPI and/or the editor(s). MDPI and/or the editor(s) disclaim responsibility for any injury to people or property resulting from any ideas, methods, instructions or products referred to in the content.